



ELSEVIER

Nuclear Physics A577 (1994) 493–510

NUCLEAR
PHYSICS A

Investigation of the $\beta\beta$ decay of ^{116}Cd into excited states of ^{116}Sn

A. Piepke ^{a,1}, M. Beck ^a, J. Bockholt ^a, D. Glatting ^a, G. Heusser ^a,
H.V. Klapdor-Kleingrothaus ^a, B. Maier ^a, F. Petry ^a, U. Schmidt-Rohr ^a,
H. Strecker ^a, M. Völlinger ^a, A.S. Barabash ^b, V.I. Umatov ^b, A. Müller ^c,
J. Suhonen ^d

^a Max-Planck-Institut für Kernphysik, P.O.Box 103980, D-69029 Heidelberg, Germany

^b Institute of Theoretical and Experimental Physics, B. Cheremushkinskaya 25, 117 259 Moscow,
Russian Federation

^c Istituto Nazionale di Fisica Nucleare, I-67010 Assergi, Italy

^d Department of Physics, University of Jyväskylä, P.O. Box 35, SF-40351 Jyväskylä, Finland

Received 3 February 1994

Abstract

The double-beta decay of ^{116}Cd into excited states of ^{116}Sn is experimentally and theoretically investigated. From an inclusive experiment, using an external source of isotopically enriched Cd, new most stringent limits for the allowed and non-standard-model decays into excited states are derived. It is further investigated whether the bremsstrahlung emitted by the $\beta\beta$ electrons can be used to derive information on the ground-state decay. For the two-neutrino-decay mode a calculation, using the quasiparticle random-phase approximation, shows that the disadvantage in phase space, in comparison to the ground-state decay, is partially compensated through the nuclear-matrix element. Experimental perspectives for other $\beta\beta$ -unstable nuclides are discussed.

Keywords: RADIOACTIVITY $^{116}\text{Cd}(2\beta)$, measured $T_{1/2}$ limits. Isotopically enriched Cd sample, low-background Ge detector. Quasiparticle RPA model calculation comparison.

1. Introduction

The investigation of the neutrinoless double-beta ($\beta\beta 0\nu$) decay is a powerful tool to search for non-zero Majorana-neutrino masses. It is one of the most sensitive tests for physics beyond the standard model (SM).

¹ Present address: California Institute of Technology 161-33, Pasadena CA 91125 USA.

Theoretically calculated nuclear-matrix elements are needed to convert experimental half-life limits, which are available for many $\beta\beta$ -unstable isotopes (see e.g. refs. [1,2]), into constraints for particle-physics parameters, such as the effective Majorana-neutrino mass and the contribution of right-handed currents to the weak interaction. It is hence essential to test the understanding of the underlying nuclear physics. The measurement of the allowed two-neutrino double-beta ($\beta\beta 2\nu$) decay gives us the possibility to study second-order weak nuclear decays. Since the calculation of $\beta\beta 2\nu$ and $\beta\beta 0\nu$ matrix elements requires substantially different theoretical methods, the measurement of the allowed decay mode cannot be considered as a rigorous test for the $\beta\beta 0\nu$ -decay channel. But on the other hand a straightforward test of theoretically calculated $\beta\beta 0\nu$ matrix elements is not known at all.

The importance of this question stimulated many experimental groups to measure $\beta\beta 2\nu$ -decay rates in different isotopes. $\beta\beta 2\nu$ -decay rates were measured in direct-counting experiments for ^{76}Ge , ^{82}Se and ^{100}Mo [3–7]. In all cases the ground-state-to-ground-state (g.s. \rightarrow g.s.) decay was investigated. The measurement of the sum-energy spectrum of the emitted electrons allowed a distinction between the different $\beta\beta$ -decay modes.

The possibility of detecting $\beta\beta$ decay into excited states of the daughter nucleus through its characteristics γ radiation did not find much attraction among the experimentalists. Only few experimental investigations of such decays are reported in the literature [8–15]. This is mainly due to the fact, that the phase space scales with $Q_{\beta\beta}^{11}$ in $\beta\beta 2\nu$ decay, where $Q_{\beta\beta}$ is the decay energy. In the case of a decay into a $J^\pi = 2^+$ state there are additional suppression mechanisms [16]. But on the other hand one has to take into account, that the detection of a structureless continuous electron spectrum in case of g.s. \rightarrow g.s. decays is more difficult than of a discrete γ line, which gives a much clearer experimental signature. Decay rates into the first excited 0^+ states of the experimentally most promising $\beta\beta$ candidates (^{96}Zr , ^{100}Mo and ^{150}Nd) were first discussed in ref. [17] together with strategies for its detection. Such inclusive experiments determine the decay rate by estimating the number of daughter nuclei created per unit time. Therefore the different $\beta\beta$ -decay modes cannot be distinguished in this way.

Also on the theoretical side only few investigations of this decay mode are known. In this article it will be shown, that the reduction of the phase space, which is available in $\beta\beta$ decay to excited states, might be partially compensated by a larger nuclear-matrix element. This finding could make the search for these decays to an attractive subject of research. For the $\beta\beta$ -unstable isotope ^{100}Mo a recent experimental investigation yielded evidence for its decay into the $J^\pi = 0^+$ level ($E_x = 1130.29$ keV) of the daughter nucleus [13]. Although we did not identify such decays in ^{116}Cd , it will be shown that the predicted half-lives have measurable magnitude.

It is well known, that the $\beta\beta 2\nu$ matrix elements show, in QRPA calculations, a strong dependence on the particle–particle interaction strength g_{pp} (see e.g. refs. [18,19]). Consequently the theoretically predicted $\beta\beta 2\nu$ half-lives can be adjusted in a wide range through this free parameter. Attempts have been made to

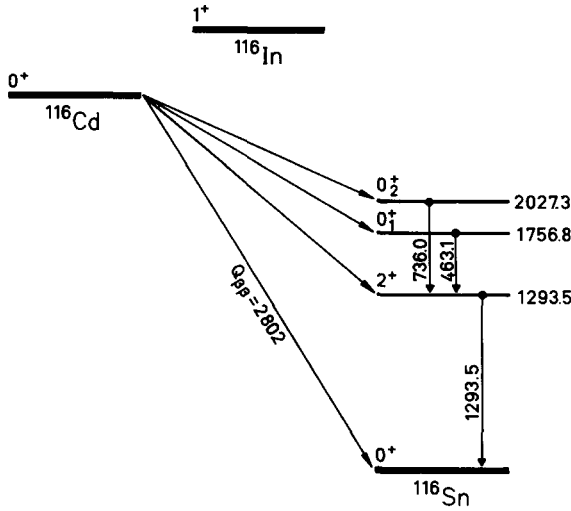


Fig. 1. Level scheme of the $\beta\beta$ decay of ^{116}Cd . Energies are denoted in keV.

overcome this ambiguity [20–22] but not undisputed solution to this problem exists yet. A recent investigation revealed [23,24], that in the case of $\beta\beta$ decays into excited levels the QRPA-matrix elements depend only weakly on g_{pp} . Their measurement is hence, within this model, a stringent test of these nuclear-structure calculations.

In experiments using thick external sources, the electrons emitted in the $\beta\beta$ decay are stopped within the source. This leads to the emission of bremsstrahlung, which might be detected as well. For $\beta\beta$ emitters with a large Q -value and a sufficiently “short” half-life, the discussed effect can have measurable strength.

In the present work the isotope ^{116}Cd has been investigated. It has a large decay energy of $Q_{\beta\beta} = 2802$ keV and its predicted half-life is one of the shortest among the 35 $\beta\beta$ -decay candidates ($T_{1/2}^{2\nu} \sim 1 \times 10^{19}$ y) [18]. Fig. 1 depicts the decay scheme of ^{116}Cd , taken from ref. [25].

An earlier experiment also studying the $\beta\beta$ decay of ^{116}Cd to excited states of ^{116}Sn found indications (on the 2σ -level) that the half-life for $\beta\beta$ decay into the $E_x = 1293.5$ keV state (a $J^\pi = 2^+$ state) could be as low as $T_{1/2}^{0^+ \rightarrow 2^+} = 6_{-2}^{+6} \times 10^{19}$ y [10]. Since the leptonic phase space is suppressed by a factor $\sim 10^5$ in comparison to the g.s. decay, this result (if indeed true) would require an unusually large nuclear-matrix element or indicate that the predicted half-life of the g.s. decay is wrong by orders of magnitude. Although a 2σ signature cannot be interpreted as serious evidence for the existence of the above decay the discussed discrepancy should be investigated in a new experiment.

2. Theoretical predictions

2.1. Formalism

The theoretical framework used in the present work consists of the use of the quasiparticle random-phase approximation theory in its charge-conserving (QRPA)

and charge-non-conserving (pnQRPA) (see e.g. refs. [26,27]) mode. The charge-conserving form of the QRPA theory uses two-quasiproton and two-quasineutron pairs to build the excited states of an even–even nucleus which, in this case, is the final nucleus in the two-neutrino double-beta decay. These excited final states can be written as QRPA phonons in the form (see e.g. ref. [28])

$$|I_k^+ M\rangle = \sum_{a \leq a'} \left[Z_{aa'}(I, k) A^\dagger(aa', IM) - W_{aa'}(I, k) \tilde{A}(aa', IM) \right] \times |\text{QRPA}\rangle, \quad (1)$$

where M labels the magnetic substates and k numbers the states for a particular angular momentum I of positive parity in order of ascending energy for the excited final states of the double-beta-decay daughter nucleus. The correlated QRPA ground state is denoted by $|\text{QRPA}\rangle$. The quasiparticle-pair-creation and annihilation operators A^\dagger and \tilde{A} are defined as

$$A^\dagger(aa', IM) = [\alpha_a^\dagger \alpha_{a'}^\dagger]_{IM}, \quad \tilde{A}(aa', IM) = -[\tilde{\alpha}_a \tilde{\alpha}_{a'}]_{IM}, \quad (2)$$

along with the definition

$$\tilde{\alpha}_a = (-1)^{j_a + m_a} \alpha_{-a}. \quad (3)$$

In the above formulae the square brackets denote angular-momentum coupling and a denotes all quantum numbers needed to specify a single-quasiparticle harmonic-oscillator state for protons ($a = p$) or neutrons ($a = n$). The quasiparticle operators α^\dagger and α have been defined introducing the Bogoliubov–Valatin transformation and performing a subsequent BCS calculation (see e.g. ref. [29]). The QRPA amplitudes $Z_{aa'}$ and $W_{aa'}$ are obtained by diagonalizing the RPA matrix [30] containing the Tamm–Dancoff two-quasiparticle submatrix and the submatrix creating the ground-state correlations into the BCS vacuum.

The pnQRPA phonons of the 1^+ states of the intermediate odd–odd nucleus are defined in a standard manner [27,31],

$$|1_m^+ M\rangle = \sum_{pn} \left[X_{pn}(1^+ m) A^\dagger(pn, 1M) - Y_{pn}(1^+ m) \tilde{A}(pn, 1M) \right] \times |\text{QRPA}\rangle, \quad (4)$$

where m is the state-enumerating index and M the magnetic quantum number. The proton–neutron quasiparticle-pair-creation and -annihilation operators A^\dagger and \tilde{A} can be inferred from Eq. (2). The amplitudes X_{pn} and Y_{pn} are obtained by diagonalizing the pnQRPA matrix [27,29,31].

The two-neutrino double-beta decay half-life $T_{1/2}^{2\nu}$ can be written as

$$\left[T_{1/2}^{2\nu}(0_{\text{g.s.}}^+ \rightarrow J_f^+) \right]^{-1} = |M_{\text{GT}}^{(2\nu)}(J_f^+)|^2 F_{\text{GT}}^{(2\nu)}(J_f^+), \quad (5)$$

where J_f^+ can either be the ground state ($0_{\text{g.s.}}^+$) or an excited state I^+ of the double-beta-decay daughter (in our case ^{116}Sn). The integrated kinematical factors

$F_{\text{GT}}^{(2\nu)}(J_f^+)$ can be calculated as described in ref. [32] and the double Gamow–Teller matrix element $M_{\text{GT}}^{(2\nu)}$ can be written in the form

$$M_{\text{GT}}^{(2\nu)}(J_f^+) = \sum_m \frac{\beta_m^+(J_f^+) \beta_m^-}{\left[\left(\frac{1}{2}Q_{\beta\beta} + E_m - M_i\right)/m_e + 1\right]^s}, \quad (6)$$

where $s = 1$ for $J = 0$ and $s = 3$ for $J = 2$, and the sum extends over all 1^+ states of the intermediate nucleus ^{116}In . The denominator of (6) consists of the energy E_m of the m th intermediate 1^+ state and the mass energy M_i of the parent nucleus, as well as of the double beta-decay Q -value, $Q_{\beta\beta}$. The different matrix elements of the half-life expression are defined as

$$\beta_m^- \equiv (1_m^+ \parallel \hat{\beta}^- \parallel 0_1^+), \quad (7a)$$

$$\beta_m^+(0^+) \equiv \sum_{m'} (0_f^+ \parallel \hat{\beta}^- \parallel 1_{m'}^+) \langle 1_{m'}^+ | 1_m^+ \rangle, \quad (7b)$$

$$\beta_m^+(2^+) \equiv \sqrt{\frac{1}{3}} \sum_{m'} (2_f^+ \parallel \hat{\beta}^- \parallel 1_{m'}^+) \langle 1_{m'}^+ | 1_m^+ \rangle, \quad (7c)$$

where the Gamow–Teller operator $\hat{\beta}^-$ reads

$$\hat{\beta}_{\text{GT}}^- = \sum_j \sigma(j) \tau^-(j). \quad (8)$$

In the above definition the isospin-lowering operator $\tau^-(j)$ converts the j th neutron into a proton and $\sigma(j)$ is the Pauli spin operator acting upon the j th nucleon. The overlap $\langle 1_{m'}^+ | 1_m^+ \rangle$ of the two 1^+ states of ^{116}In coming from the two different pnQRPA calculations (one for ^{116}Cd and the other for ^{116}Sn) has a stabilizing effect upon the matrix element $M_{\text{GT}}^{(2\nu)}$ [19] and is given by

$$\langle 1_{m'}^+ | 1_m^+ \rangle = \sum_{\text{pn}} \left[X_{\text{pn}}(1^+ m') \bar{X}_{\text{pn}}(1^+ m) - Y_{\text{pn}}(1^+ m') \bar{Y}_{\text{pn}}(1^+ m) \right], \quad (9)$$

where the barred (unbarred) amplitudes come from the pnQRPA calculation based on ^{116}Sn (^{116}Cd).

In the present calculation the final state 0_f^+ can either be the ground state or the 0^+ two-phonon state, whereas the final state 2_f^+ can either be the first 2^+ state or the 2^+ two-phonon state. If the final state is $0_{\text{g.s.}}^+$, then the calculation of the reduced matrix element of Eq. (7b) is simple and the corresponding detailed expression is given e.g. in ref. [29] (the expression corresponding to (7a) is also given there). In the case of an excited state I^+ , the expressions for the reduced matrix elements of (7b) and (7c) are more complicated and given in detail in ref. [28] for a one-phonon QRPA excitation and in ref. [24] for a two-phonon QRPA excitation. It may be noted that our two-phonon expressions are similar to the ones quoted in ref. [33].

2.2. Numerical calculation and results

The double-beta calculations have been performed in two different sets of harmonic-oscillator single-particle orbitals. The first set contained the $3\hbar\omega$ and

$4\hbar\omega$ harmonic-oscillator major shells as well as the intruder orbital $0h_{11/2}$ from the $5\hbar\omega$ shell, both for protons and neutrons. The second set contained, in addition to the contents of the first set, the complete $5\hbar\omega$ major shell and the $0i_{13/2}$ intruder from the $6\hbar\omega$ shell for neutrons. For protons the single-particle orbitals of the first set were used. These two single-particle sets served as a test of the convergence of the calculated electric and beta-decay observables. The convergence turned out to be good since both the $B(E2)$ and the double-beta results were practically the same in the two basis sets. The experimental $B(E2; 2_1^+ \rightarrow 0_{g.s.}^+)$ for ^{116}Sn could be reproduced with proton and neutron effective charges near unity.

The nucleon–nucleon interaction was taken to be the G-matrix interaction derived from the Bonn one-boson-exchange potential [34]. The magnitude of the oscillator parameter was determined as discussed in ref. [35]. The monopole matrix elements were used in calculating the BCS ground state of ^{116}Cd and ^{116}Sn . The overall magnitude of these proton- (neutron-) pairing-matrix elements were adjusted by comparing the calculated pairing gaps with the corresponding semi-empirical pairing gaps obtained from the tabulated separation energies [36] for protons (neutrons).

The overall strength of the proton–proton and neutron–neutron quadrupole G-matrix elements was adjusted in the QRPA calculation to yield the experimental energy of the first 2^+ state in ^{116}Sn . The proton–neutron-interaction G-matrix elements, coupled to angular momentum $J = 1$, appear in the pnQRPA calculation. These matrix elements can be renormalized separately for the particle–particle and particle–hole channels. The strength of the particle–hole channel was adjusted to yield the energy of the Gamow–Teller giant-resonance state (GTGR) in ^{116}In . The effect of the proton–neutron particle–particle channel upon the beta- and double-beta-decay observables has been discussed extensively in the literature during the recent past [19,29,31,37–39]. In the case of the double-beta decay of ^{116}Cd , the magnitude of the g.s. \rightarrow g.s. matrix element is a rather slowly varying function of the scaling parameter g_{pp} of the particle–particle interaction strength. According to previous experience the best theoretical estimates for the double-beta half-lives occur for g_{pp} -values near unity, corresponding to a pure G-matrix interaction.

In the present study, g_{pp} -values near $g_{pp} = 1$ would correspond to a half-life of $T_{1/2}^{2\nu}(0_{g.s.}^+ \rightarrow 0_{g.s.}^+) \approx 1.2 \times 10^{19}$ y ($M_{GT}^{(2\nu)} \approx 0.10$ in Eq. (6)) which is rather close to the recently measured value of $2.2_{-0.4}^{+0.7} \times 10^{19}$ y by the ELEGANTS V collaboration [40]. The theoretical transition rates to the excited states of ^{116}Sn depend only very weakly on the particle–particle interaction strength [23,24]. The predicted theoretical half-lives, for $g_{pp} \approx 1$, read (in parenthesis we display the value of the corresponding transition-matrix element according to Eq. (6))

$$T_{1/2}^{2\nu}(0_{g.s.}^+ \rightarrow 2_1^+) \approx 2.0 \times 10^{23} \text{ y} \quad (M_{GT}^{(2\nu)} \approx -0.030),$$

$$T_{1/2}^{2\nu}(0_{g.s.}^+ \rightarrow 0_{2-ph}^+) \approx 1.6 \times 10^{22} \text{ y} \quad (M_{GT}^{(2\nu)} \approx -0.56),$$

where the two-phonon 0^+ state, 0_{2-ph}^+ , is taken to lie at the excitation energy of 2027 keV as suggested by the analysis of Raman et al. [41]. The transition rate to

$J_f^+ = 2_{2-ph}^+$ is strongly suppressed by the phase space and thus far beyond the reach of the present-day experimental techniques.

3. Experiment

3.1. The source

811 g of isotopically enriched metallic Cd were used to study its $\beta\beta$ -decay features. The average isotopical abundance of the $\beta\beta$ -unstable ^{116}Cd is 87% whereas the natural abundance is 7.5%. Approximately 3.7×10^{24} ^{116}Cd nuclei were exposed to the detection efficiency. The Cd sample is composed of 13 pieces of different shape, weight and isotopical composition. These pieces were placed around the endcap of a low-background Ge detector.

3.2. The detector

A HP Ge detector of 900 g active mass has been used to detect the γ radiation resulting from $\beta\beta$ decay into excited nuclear states of the daughter nucleus. Since the expected decay rates are small, the background of the detection system has to be very low. The Ge crystal is mounted in a special low-background cryostat. The crystal holder is made from Al (supplier: Vereinigte Aluminium Werke of Grevenbroich, Germany). The supplier specified ^{232}Th and ^{238}U concentrations of less than 30 and 43 ppt, respectively.

The vacuum endcap is made of zone refined Si (obtained from Wacker-Chemitronic of Burghausen, Germany) with ^{232}Th and ^{238}U concentrations of less than 0.1 and 2 ppt, respectively. The extremely high purity of this material is also reflected by its specific resistivity which is larger than $1000 \Omega \cdot \text{cm}$.

The rest of the cryostat is made of electrolytical Cu obtained directly from the producer (Norddeutsche Affinerie of Hamburg, Germany) in order to minimize its exposure time to the cosmic radiation and hence its activation. Screws were made of pre-WW-I ships steel, which is free of ^{60}Co . Special care was taken to minimize the influence of surface contaminations on the background. All cryostat parts were etched (the Cu parts with HNO_3 , the Al and Si with NaOH). The cryostat was assembled in a cleanroom. The cryostat parts were joint by electron-beam welding to avoid soldering. The preamplifier including its first stage (FET) is mounted outside the shield.

The detector has an intrinsic energy resolution (FWHM) of 2.3 keV at 1.332 MeV. It is mounted in a passive shield composed of 24 cm electrolytical Cu and 20 cm Pb (supplier Boliden, Sweden). The setup is covered by an airtight steel box which is flushed by N_2 gas to remove the radioactive Rn gas from the inner cavities of the shield. Radioactive sources mounted on steel wires can be fed through the shield for weekly calibration measurements. In this way the stability of the signal-processing electronics and detector performance is monitored. The setup is

located in the Gran Sasso underground laboratory in Italy. The shielding thickness of 3500 m w.e. reduces the cosmic radiation effectively. The integral counting rate (100–2700 keV) of the spectrometer is 18.3 counts/keV · y · kg.

3.3. Efficiency estimation

To calculate the photopeak efficiency of the photons, emitted in the decay of the excited states of ^{116}Sn , and the total efficiency of bremsstrahlung, caused by $\beta\beta$ electrons, a Monte Carlo programme based on the CERN code GEANT3.14 has been applied. To verify the accuracy of the programme, several calibrated radioactive sources (^{238}U , ^{137}Cs and ^{60}Co) were measured on the surface of the detector vacuum endcap. By the area of the measured γ lines of the different sources, efficiency values can be calculated for the corresponding photon energies. An efficiency curve was obtained by fitting a double-logarithmic polynome to the data points. In the energy range from 200 to 2650 keV, simulated and measured efficiency curves agree within 5%. The efficiency estimation was confirmed by an independent calculation done at ITEP.

The absolute detection efficiency and the shape of bremsstrahlung caused by the $\beta\beta$ electrons was calculated separately for the 2ν and the 0ν mode by the Monte Carlo programme. For this simulation the sum energy of the $\beta\beta$ electrons was distributed to equal parts among both electrons. For the 2ν mode the sum energy for the electrons of one decay was randomly chosen according to the well-known sum-energy distribution of $\beta\beta$ electrons [16]. Fig. 2 shows the simulated bremsstrahlung spectra of $\beta\beta 2\nu$ and $\beta\beta 0\nu$ decay together with that resulting from the β decay of ^{90}Sr .

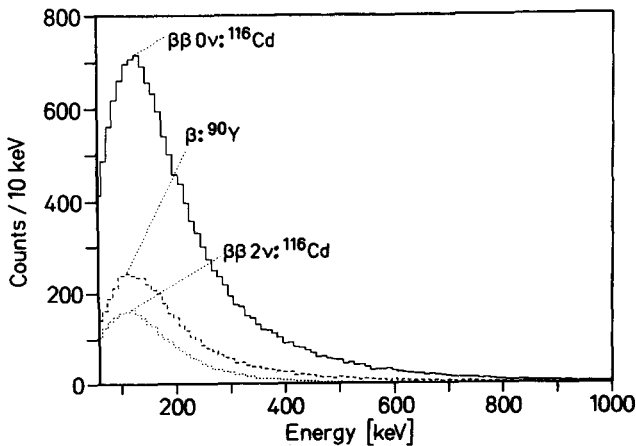


Fig. 2. Simulated bremsstrahlung spectra of different double- and single-beta decays. 1 million decays were simulated. The integral and therefore detection efficiency is mainly determined by the Q -value of the decay. The channel width is 10 keV.

4. Data taking

The Cd sample was measured during 119.47 days. Then the probe was removed and the detector background measured during 228.77 days. The complete set of data corresponds to 413.8 real-time days. During this time 59 calibration measurements with ^{60}Co and ^{228}Th sources were performed. The relative variation of the bin width was $\pm 2.2 \times 10^{-3}$ over the full measuring period. These shifts in the energy calibration were software-corrected, resulting in a long-term energy resolution of 2.65 and 3.42 keV at 1.332 MeV for the sample- and blank-measurement, respectively. Since the sample- and blank-experiments were preceded by another blank run of 228 days in which the detector was shielded by 30 cm of Pb, it could be excluded that the experimental background is mainly caused by the Cu shield. Hence it is not necessary to correct for the mass absorption of the Cd sample when subtracting the background. The data were taken in an event-by-event mode, using 13-bit ADCs.

5. Data analysis

(1) In our analysis, first the existence of the γ lines, which are characteristic for the $\beta\beta$ decay of ^{116}Cd into excited states of ^{116}Sn , is tested. All counting-rate limits were deduced using the method recommended by the Particle Data Group for a Poisson-distributed signal superimposed to background.

(2) In a second step, limits are derived for the g.s. \rightarrow g.s. $\beta\beta$ decay. These limits are based on a comparison between the measured continuous net-spectrum and the bremsstrahlung spectra of the $\beta\beta$ electrons.

(3) The background caused by radioactive impurities of the shield and detector cryostat can be removed by subtracting the measured background from the probe-spectrum. The background caused by contaminations of the Cd sample cannot be taken into account by this procedure. Thus we unfold the probe-related background by a Monte Carlo simulation in order to increase the sensitivity for the detection of bremsstrahlung continua. This needs a detailed understanding of the background composition.

5.1. $\beta\beta$ decay into excited states

As can be seen in the level scheme of ^{116}Sn , depicted in Fig. 1, the decay of the excited 2^+ , 0_1^+ and 0_2^+ states are resulting in the emission of γ quanta with $E_\gamma = 1293.5$, 463.1 and 736 keV. The absolute peak efficiency is 9.85×10^{-3} , 1.67×10^{-2} and 1.36×10^{-2} , respectively. Fig. 3 shows the measured spectra around the above energies.

5.1.1. Decay into the $E_x = 1293.5$ keV state

Since no peak at $E_\gamma = 1293.5$ keV can be found in the probe-experiment, 3.46(1.75) (90(68)% c.l.) $\beta\beta$ events are excluded by linearly interpolating the low- and high-energetic background next to the 3σ -peak interval. This corresponds to a

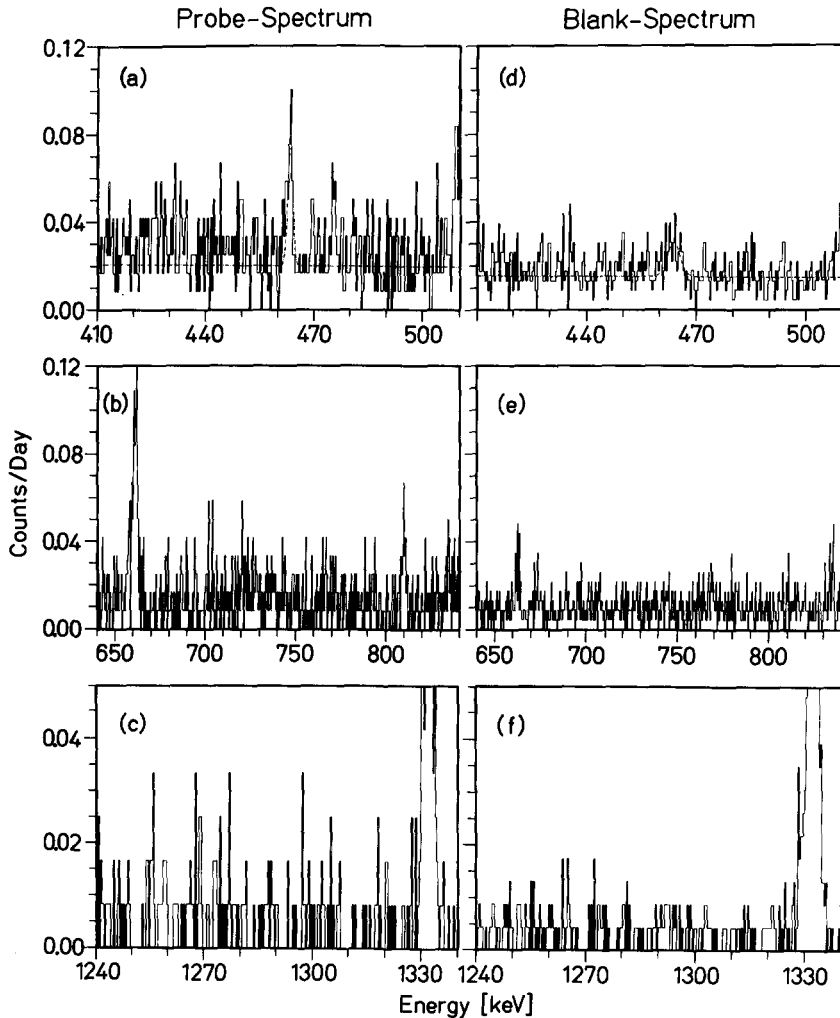


Fig. 3. Measured spectra of probe- and blank-runs around the different $\beta\beta$ -decay energies. The channel width is 0.36 keV. The fits of the γ peaks at 463.1 keV are shown as dotted lines.

half-life limit of: $T_{1/2}^{0^+ \rightarrow 2^+} > 2.37(4.69) \times 10^{21}$ y with 90(68)% c.l.. The described analysis is based on the assumption, that the true spectral shape is a flat continuum. If the blank-measurement is used to estimate the number of background events in the 3σ -peak interval we get a very similar result of $T_{1/2}^{0^+ \rightarrow 2^+} > 2.06(3.97) \times 10^{21}$ y with 90(68)% c.l.. In the latter analysis it is assumed, that the background is not source-related.

5.1.2. Decay into the $E_x = 1756.9$ keV state

We find a clear peak at $E_\gamma = 463.3 \pm 0.3$ keV in the sample-spectrum, which has a peak counting rate of 0.28 ± 0.07 cpd. A background fluctuation of 5.3σ

would be necessary to explain this structure. On the other hand it is well known, that such a peak should occur in the decay of ^{228}Ac ; a member of the ^{232}Th -decay series. In the blank-spectrum we also find a peak at this energy, with a peak counting rate of 0.19 ± 0.05 cpd. Both peak counting rates agree within 1σ , which shows that the discussed line is not source-related and can therefore not be interpreted as evidence for $\beta\beta$ decay. These two values yield a half-life limit of $T_{1/2}^{0^+ \rightarrow 0^+} > 7.3(10.0) \times 10^{20}$ y with 90(68)% c.l..

The probability that the $E_x = 1756.9$ keV state decays directly via internal conversion into the ground state is only 0.29%. This means, that the same intensity (efficiency-corrected) measured in the $E_\gamma = 463.1$ keV line should become observable in the $E_\gamma = 1293.5$ keV peak. Hence we can apply the half-life limit measured through the $E_\gamma = 1293.5$ keV peak also to $\beta\beta$ decays into the 0_1^+ state. Taking into account small efficiency losses due to coincidence summation we get in this way $T_{1/2}^{0^+ \rightarrow 0^+} > 2.05(4.05) \times 10^{21}$ y with 90(68)% c.l..

On the other hand it should also be mentioned that the intensity of the 463.3 keV line cannot be understood on the basis of the other ^{232}Th lines present in the measured spectrum. Under the assumption that the 463.3 keV peak is caused by $\beta\beta$ decay while the coincident 1293.5 keV peak is absent due to statistical reasons, we derive a probability of $\sim 10^{-4}$ for this hypothesis.

5.1.3. Decay into the $E_x = 2027.3$ keV state

From the absence of a peak at $E_\gamma = 736$ keV a half-life limit of $T_{1/2}^{0^+ \rightarrow 0^+} > 7.07(10.64) \times 10^{20}$ y with 90(68)% c.l. can be determined. Because also here a direct decay into the g.s. is not possible we get $T_{1/2}^{0^+ \rightarrow 0^+} > 2.05(4.05) \times 10^{21}$ y with 90(68)% c.l. by using the same argument as above.

5.2. $\beta\beta$ decays into the ground state

As already explained earlier, the bremsstrahlung emitted by the $\beta\beta$ -decaying Cd source can be used to derive limits for g.s. \rightarrow g.s. decays. While the deduction of half-life limits is straightforward, a direct measurement of $\beta\beta$ decay would be more difficult, since the spectral shape of the bremsstrahlung continua is not very different for single- and double-beta decays.

In this analysis only continuous components of the measured spectra are of interest. We thus removed 23 strong peaks from these spectra. Then the continuous blank-spectrum was subtracted from the probe spectrum. Fig. 4 shows the probe-blank- and resulting net-spectrum. For the analysis an evaluation interval which extends from 60 to 230 keV is used. It contains the maxima of both continua. The detection efficiencies can be determined from the simulated bremsstrahlung continua for the above mentioned interval to be 9.78×10^{-3} and 2.09×10^{-3} for the 0ν - and 2ν -decay mode, respectively. In the net-spectrum $N_c = 2995$ counts are contained in the evaluation interval. The excluded number of events ΔN_c is defined by

$$\Delta N_c < N_c + n\sqrt{N_p + N_b}. \quad (10)$$

Here n connects the limit to a confidence level. If a Gauss distribution is assumed $n = 1.28(0.47)$ for 90(68)% c.l.. N_b and N_p are the number of events in the evaluation interval of the blank- and probe-measurement, respectively.

By this procedure we get the following results:

2ν decay g.s. \rightarrow g.s.: $T_{1/2}^{2\nu} > 5.5(5.7) \times 10^{17}$ y with 90(68)% c.l.,

0ν decay g.s. \rightarrow g.s.: $T_{1/2}^{0\nu} > 2.6(2.7) \times 10^{18}$ y with 90(68)% c.l.

The apparent “bump” in the net-spectrum, shown in Fig. 4, looks very similar to the shape of the simulated bremsstrahlung spectra.

5.3. Background analysis

The good energy resolution and hence high diagnostic power of the Ge detector allows to identify those activities located in the Cd sample through the differences of the γ -peak counting rates of the probe- and blank-measurement. ^{40}K , ^{110}Ag and ^{137}Cs contaminations of the Cd probe were identified with statistical significances of 8.4σ , 3.2σ and 7.3σ , respectively. All other counting-rate differences show significances lower than 3σ .

The γ spectra of the above activities were modelled through the use of the described Monte Carlo programme. This treatment included the γ radiation as well as the bremsstrahlung emitted by the stopped β electrons. The correct shapes of the electron spectra were used in this model, taking into account that the above isotopes undergo forbidden β decays. The normalization of the simulated to measured net-peak areas yields absolute activities of ^{40}K : 14.8 ± 2 mBq/kg, ^{110}Ag : 0.4 ± 0.1 mBq/kg and ^{137}Cs : 0.8 ± 0.1 mBq/kg. The discussed method, however, has the disadvantage that only those activities having a γ branch can be treated quantitatively.

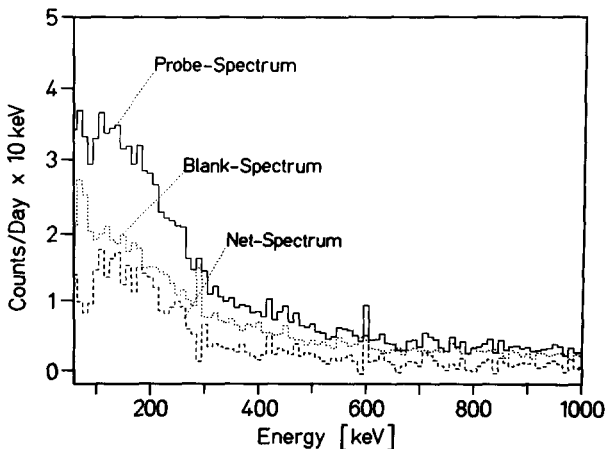


Fig. 4. Continuous components of measured probe- and blank-spectra. Peaks were removed. The background-subtracted net-spectrum shows that there are additional source-related background components. The bin width is 10 keV.

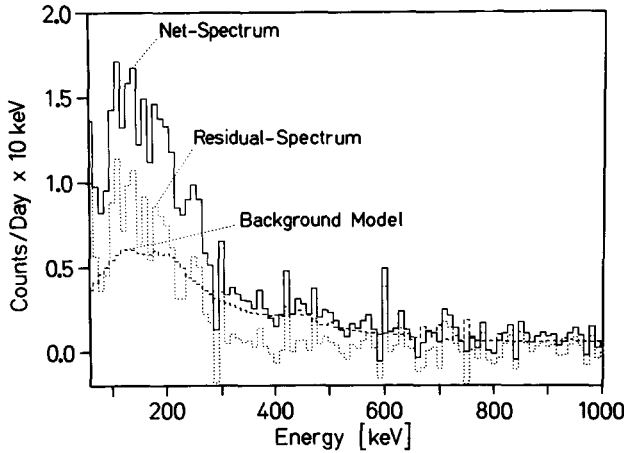


Fig. 5. Continuous net-spectrum and the Monte Carlo background model, which is constructed from a quantitative measurement of the different background components. The good agreement at energies above ~ 400 keV indicates, that the residual background is not due to Compton scattering of high-energetic γ rays. The shape of the residual spectrum is very similar to that expected for bremsstrahlung.

Fig. 5 depicts the measured continuous net-spectrum together with the continuous part of the discussed background model. After subtracting the background model, $N_c = 1848$ counts are contained in the evaluation interval of the residual-spectrum. The number of excluded counts can be estimated through

$$\Delta N_c < N_c + n\sqrt{N_p + N_b + N_{\text{mod}}}, \quad (11)$$

where N_{mod} is the number of events contained in the evaluation interval of the background model. The corresponding half-life limits are
 2ν decay g.s. \rightarrow g.s.: $T_{1/2}^{2\nu} > 8.7(9.1) \times 10^{17}$ y with 90(68)% c.l.,
 0ν decay g.s. \rightarrow g.s.: $T_{1/2}^{0\nu} > 4.1(4.3) \times 10^{18}$ y with 90(68)% c.l.

As can be seen in Fig. 5 the discussed background model explains only 62% of the events in the evaluation interval. Since the detection of bremsstrahlung is not very selective on the shape of the initial electron spectrum, these events could also be due to a long-lived β activity without γ branch. A simulated ^{90}Sr activity of 61 mBq/kg, corresponding to a concentration of only 10^{-17} g/g, would fit quite well. Due to its small Q -value of only 322 keV, the bremsstrahlung emitted by the β -unstable isotope ^{113}Cd does not resemble the spectral shape of the residual-spectrum. Its isotopical abundance has been measured by mass spectroscopy to be $\approx 1\%$. Because of the small emission probability of bremsstrahlung and the extremely long half-life of ^{113}Cd (9×10^{15} y) it contributes only $\approx 1\%$ to the extra events of the residual-spectrum.

The sensitivity of the setup can be estimated by subtracting the hypothetical ^{90}Sr activity, which might be quantitatively measured in an independent experiment. The sensitivity would then only be limited by the fluctuation of the residual

Table 1

Activity limits deduced for the different construction materials and the Cd sample. The limits for the latter material were deduced from the difference of probe- and blank-data, while the results for the others were derived from the blank-run alone. The large differences in sensitivity are due to the different amounts of material used in the experiment, indicated in the last line of the table. For the natural-decay series, secular equilibrium was assumed

Isotope	Activity (mBq/kg)			
	Cd	Al	Si	Cu
^{40}K	–	4.5	3.2	0.28
^{60}Co	0.3	3.4	2.5	0.11
^{137}Cs	–	0.3	0.3	0.02
^{232}Th	0.6	2.1	1.7	0.08
^{238}U	0.7	2.4	1.9	0.13
Mass (kg)	0.811	0.174	0.485	255

background. In that case it can be estimated to be $T_{1/2}^{2\nu} > 5 \times 10^{18}$ y; not too far from the positive result of ref. [40]. The actually achieved sensitivity is clearly limited by the radiopurity of the Cd sample.

The background analysis can also be used to derive purity information for the construction materials of the detector, the shield and the Cd probe. A conservative approach has been chosen in which the simulated spectra of each material and radioactive isotope were normalized on the measured peak areas. Consequently it was assumed, that the measured background is caused by one material alone. In the case of the ^{232}Th and ^{238}U decay chains no indication for a disequilibrium was found. The corresponding activities were calculated as the average over all associated peak intensities. Table 1 contains the activity limits for Cd, Al, Si and Cu. In addition a ^{207}Bi contamination of 1.0 ± 0.09 mBq/kg was found in the Al.

6. Discussion

If the excess of events in the difference of probe- and blank-measurement, discussed in ref. [10], would be due to $\beta\beta$ decay into the $E_x = 1293.5$ keV level of ^{116}Sn , we should expect a peak of 137 counts at $E_\gamma = 1293.5$ keV in the described experiment. Since we find, after 119.5 days of counting, only six events in the 99% interval around this energy, it has to be concluded by this 55.9σ -disagreement, that the signal of ref. [10] cannot be caused by $\beta\beta$ decay.

Because the authors of ref. [10] did not find the characteristic γ line at $E_\gamma = 1293.5$ keV in the probe spectrum, they also quoted a half-life limit of $T_{1/2} > 1.7 \times 10^{20}$ y with 68% c.l.. The result of this new investigation represents therefore a 23-fold improvement with respect to these older data.

In Table 2 the experimental limits for the half-lives of the $\beta\beta$ decay of ^{116}Cd into excited states of ^{116}Sn are compared with the theoretical predictions and the most stringent limits found in the literature. From this compilation it is clear, that

Table 2

Comparison of the calculated nuclear-matrix elements ($M_{GT}^{2\nu}$) and expectations for the half-lives ($T_{1/2}^{2\nu}$) with the experimental results ($T_{1/2}^{0\nu+2\nu}$). The most stringent experimental limits for the decays into excited states reported in the literature are shown in the two right columns. All limits have 90% c.l. with exception of that marked ^c, which has 68% c.l. The value for the $\beta\beta 2\nu$ decay into the g.s. (marked ^b) is not a limit but a measurement. ϵ denotes the calculated γ -detection efficiency

E_x (keV)	J^π (\hbar)	E_γ (keV)	ϵ (%)	$M_{GT}^{2\nu}$	$T_{1/2}^{2\nu}$ (y)	$T_{1/2}^{0\nu+2\nu}$ (y)	$T_{1/2}^{0\nu}$ (y)	$T_{1/2}^{2\nu}$ (y)
0	0^+	–	–	0.10	1.2×10^{19}	–	1.0×10^{22} ^a	$2.2_{-0.4}^{+0.7} \times 10^{19}$ ^b
1293.5	2^+	1293.5	0.99	–0.03	2.0×10^{23}	2.3×10^{21}	1.6×10^{21} ^a	1.7×10^{20} ^c
1756.8	0^+	463.1	1.67	–	–	2.0×10^{21}	4.2×10^{20} ^a	8.1×10^{18} ^a
2027.3	0^+	736	1.36	–0.56	1.6×10^{22}	2.0×10^{21}	3.2×10^{20} ^a	9.4×10^{18} ^a

^a Taken from ref. [11].

^b Taken from ref. [40].

^c Inclusive result taken from ref. [10].

the discussed inclusive results represent the most stringent experimental information on both the allowed and non-standard-model decay modes into excited states. Those half-life limits denoted with ^a were derived from an experiment using CdWO₄ scintillators (made of enriched Cd) simultaneously as source and detector for the $\beta\beta$ electrons [11]. Their limits for the g.s. decays are, however, orders of magnitude more stringent. On the other hand, it is quite interesting that the relatively simple detection of bremsstrahlung is only a factor ~ 25 less sensitive than the sophisticated ELEGANTS V setup [40]. Their measured value for the half-life of the $\beta\beta 2\nu$ decay into the ground state is marked ^b in Table 2.

The theoretical predictions listed in Table 2 show that the nuclear-matrix element of the $E_x = 2027.3$ keV level is significantly larger than that of the g.s. decay. The resulting half-life is still one order of magnitude larger than the experimental limit.

Unfortunately a half-life prediction was not possible for the $E_x = 1756.8$ keV state. If one assumes a similar matrix element as for the g.s. decay the resulting half-life should be $T_{1/2}^{2\nu} \approx 4.3 \times 10^{22}$ y, while a matrix element of the same magnitude as for the $E_x = 2027.3$ keV level would lead to $T_{1/2}^{2\nu} \approx 1.4 \times 10^{21}$ y. The latter value is very close to the achieved experimental sensitivity and indeed measurable.

In order to find out whether half-lives of the order of several 10^{22} y are measurable a Monte Carlo simulation was performed. If 5 kg of high-purity source material in an optimized geometry would be used together with one of the large enriched detectors of the Heidelberg–Moscow collaboration [1] a ~ 12.3 -fold improvement in the sensitivity (for the $E_\gamma = 1293$ keV line) compared to the described experiment can be expected. The decay into the $E_x = 2027.3$ keV level should become visible through the $E_\gamma = 1293.5$ keV peak within half a year of measurement. The $\beta\beta 2\nu$ decay into the g.s. could become visible within 1–2 years of data taking. Since a six-fold increase of the source strength is not very realistic due to fiscal reasons, also other isotopes were studied.

Besides ^{100}Mo , which has already been studied in detail [13,14], there are two other promising nuclides, which have the advantage of large decay energies: ^{96}Zr and ^{150}Nd with $Q_{\beta\beta} = 3350$ and 3367 keV. The excitation energies of $E_x = 1147.9$ and 740.4 keV of their first $J^\pi = 0^+$ states are resulting in moderate reductions in phase space by factors 39.37 and 9.01, respectively. The predicted g.s.-decay half-lives of $T_{1/2}^{2\nu} = 1 \times 10^{19}$ and 7×10^{18} y are also relatively short [18]. If the matrix elements of the decays into these 0^+ states are similar to those of the g.s. decays we can expect half-lives of $T_{1/2}^{2\nu} \sim 4 \times 10^{20}$ and 7×10^{19} y. The excited nuclear levels populated in those decays show high γ -emission probabilities (100% and 98%, respectively). If the matrix element for the $\beta\beta$ decay of ^{150}Nd into the first excited 0^+ state of ^{150}Sm (a two-phonon state as in the case of ^{116}Sn [42]) would show a similar enhancement over that of the g.s. decay as found for ^{116}Cd , the decay rate into this excited level could even exceed that of the g.s. decay!

Using 1 kg of isotopically enriched source material in an optimized geometry the Monte Carlo simulation yields improvement factors of 1.9 and 2.6 (in comparison to the result obtained through the $E_\gamma = 463$ keV line of the ^{116}Cd decay) for the discussed detector and the large enriched detector, respectively. Assuming a similar radiopurity of the source material as found for the Cd sample the discussed decays should hence become observable when using the setup described in this article. If 5 kg of enriched Nd would be used also the g.s. decay could be observable through the bremsstrahlung (improvement factor for the efficiency ~ 8.3) if the large enriched detector is used.

7. Conclusion

New most stringent experimental half-life limits for the $\beta\beta$ decay of ^{116}Cd into excited states of ^{116}Sn are derived using an isotopically enriched Cd sample and a low-background Ge detector. Estimates of the decay rates are obtained through a QRPA calculation. These calculations show that the disadvantage in phase space compared to the g.s. decay is partially compensated through a larger nuclear-matrix element. It has been shown that such transitions are, in principle, accessible by the use of low-level γ spectroscopy.

References

- [1] A. Balysh, M. Beck, S.T. Belyaev, J. Bockholt, A. Demehin, J. Echternach, A. Gurov, G. Heusser, M. Hirsch, H.V. Klapdor-Kleingrothaus, I. Kondratenko, V.I. Lebedev, B. Maier, A. Müller, F. Petry, A. Piepke, U. Schmidt-Rohr, H. Strecker and K. Zuber, Phys. Lett. B283 (1992) 32
- [2] J.-C. Vuilleumier, J. Busto, J. Farine, V. Jörgens, L.W. Mitchell, M. Treichel, J.-L. Vuilleumier, H.T. Wong, F. Boehm, P. Fisher, H.E. Henrikson, D.A. Imel, M.Z. Iqbal, B.M. O'Callaghan-Hay, J. Thomas and K. Gabathuler, Phys. Rev. D48 (1993) 1009
- [3] A. Balysh, M. Beck, S.T. Belyaev, F. Bensch, J. Bockholt, A. Demehin, A. Gurov, G. Heusser, H.V. Klapdor-Kleingrothaus, I. Kondratenko, D. Kotelnikov, V.I. Lebedev, B. Maier, A. Müller, F. Petry, A. Piepke, A. Pronskey, H. Strecker, M. Völlinger and K. Zuber, Phys. Lett. B322 (1994)

- [4] F.T. Avignone III, R.L. Brodzinski, C.K. Guerard, I.V. Kirpichnikov, H.S. Miley, V.S. Pogosov, J.H. Reeves, A.S. Starostin and A.G. Tamanyan, *Phys. Lett.* B256 (1991) 559
- [5] S.R. Elliott, A.A. Hahn and M.K. Moe, *Phys. Rev. Lett.* 59 (1987) 2020
- [6] S.R. Elliott, M.K. Moe, M.A. Nelson and M.A. Vient, *J. of Phys.* G17 (1991) S145
- [7] H. Ejiri, K. Fushimi, T. Kamada, H. Kinoshita, H. Kobiki, H. Ohsumi, K. Okada, H. Sano, T. Shibata, T. Shima, N. Tanabe, J. Tanaka, T. Taniguchi, T. Watanabe and N. Yamamoto, *Phys. Lett.* B258 (1991) 17
- [8] E.B. Norman and D.M. Meekhof, *Phys. Lett.* B195 (1987) 126
- [9] E. Bellotti, E. Fiorini, C. Liguori, A. Pullia, A. Sarracino and L. Zanotti, *Lett. Nuovo Cimento* 33 (1982) 273;
E. Bellotti, C. Cattadori, O. Cremonesi, E. Fiorini, C. Liguori, A. Pullia, P.P. Sverzellati and L. Zanotti, *Europhys. Lett.* 3 (1987) 889
- [10] A.S. Barabash, A.V. Kopylov and V.I. Cherehovskiy, *Phys. Lett.* B249 (1990) 186
- [11] F.A. Danevich, V.V. Kobychev, V.N. Kouts, V.I. Tretyak and Yu. Zdesenko, *Proc. 3rd Int. Symp. on weak and electromagnetic interactions in nuclei, Dubna 1992*, ed. Ts.D. Vylov (World Scientific, Singapore, 1992) p. 575
- [12] M. Beck, J. Bockholt, J. Echternach, G. Heusser, M. Hirsch, H.V. Klapdor-Kleingrothaus, A. Piepke, H. Strecker, K. Zuber, A. Bakalyarov, A. Balysh, S.T. Belyaev, A. Demehin, A. Gurov, I. Kondratenko, V.I. Lebedev, A. Pronsky and A. Müller, *Z. Phys.* A343 (1992) 397
- [13] A.S. Barabash, F.T. Avignone III, C.K. Guerard, R.L. Brodzinski, H.S. Miley, J.H. Reeves and V.I. Umatov, *Proc. 3rd Int. Symp. on weak and electromagnetic interactions in nuclei, Dubna 1992*, ed. Ts.D. Vylov (World Scientific, Singapore, 1992) p. 582
- [14] D. Blum, J. Busto, J.E. Campagne, D. Dassié, F. Hubert, Ph. Hubert, M.C. Isaac, C. Izac, S. Jullian, V.N. Kouts, B.N. Kropivnyansky, D. Lalanne, T. Lamhamdi, F. Laplanche, F. Leccia, I. Linck, C. Longuemare, P. Mennrath, F. Natchez, F. Scheibling, G. Szklarz, V.I. Tretyak and Yu.G. Zdesenko, *Phys. Lett.* B275 (1992) 506
- [15] N. Kudomi, H. Ejiri, K. Nagata, K. Okada, T. Shibata, T. Shima and J. Tanaka, *Phys. Rev.* C46 (1992) R2132
- [16] W.C. Haxton and G.J. Stephenson Jr., *Part. Nucl. Phys.* 12 (1984) 409
- [17] A.S. Barabash, *JETP Lett.* 51 (1990) 207
- [18] A. Staudt, K. Muto and H.V. Klapdor-Kleingrothaus, *Europhys. Lett.* 13 (1990) 31
- [19] O. Civitarese, A. Faessler and T. Tomoda, *Phys. Lett.* B194 (1987) 11
- [20] X.R. Wu, A. Staudt, H.V. Klapdor-Kleingrothaus, C. Ching and T. Ho, *Phys. Lett.* B272 (1991) 169
- [21] X.R. Wu, A. Staudt, T.T.S. Kuo and H.V. Klapdor-Kleingrothaus, *Phys. Lett.* B276 (1992) 274
- [22] M. Hirsch, X.R. Wu, H.V. Klapdor-Kleingrothaus, C. Ching and T. Ho, *Z. Phys.* A345 (1993) 163; *Phys. Reports*, in press
- [23] J. Suhonen and O. Civitarese, *Phys. Lett.* B308 (1993) 212
- [24] O. Civitarese and J. Suhonen, *Nucl. Phys.* A575 (1994) 251
- [25] C.M. Lederer and V.S. Shirley, *Table of isotopes*, 7th Ed. (Wiley, New York, Chichester, Brisbane, Toronto, 1978)
- [26] K. Muto, E. Bender and H.V. Klapdor, *Z. Phys.* A333 (1989) 125;
K. Muto and H.V. Klapdor, *Neutrinos*, ed. H.V. Klapdor (Springer, Heidelberg, New York, 1988) p. 183
- [27] K. Muto, E. Bender, T. Oda and H.V. Klapdor-Kleingrothaus, *Z. Phys.* A341 (1992) 407
- [28] J. Suhonen, *Nucl. Phys.* A563 (1993) 91
- [29] J. Suhonen, T. Taigel and A. Faessler, *Nucl. Phys.* A486 (1988) 61
- [30] M. Baranger, *Phys. Rev.* 120 (1960) 957
- [31] P. Vogel and M.R. Zirnbauer, *Phys. Rev. Lett.* 57 (1986) 3148
- [32] M. Doi, T. Kotani and E. Takasugi, *Prog. Theor. Phys. Suppl.* 83 (1985) 1
- [33] A. Griffiths and P. Vogel, *Phys. Rev.* C46 (1992) 181
- [34] K. Holinde, *Phys. Reports* 68 (1981) 121
- [35] G.F. Bertsch, *The practitioner's shell model* (North-Holland, Amsterdam, 1972)
- [36] A.H. Wapstra and G. Audi, *Nucl. Phys.* A432 (1985) 1
- [37] K. Muto, E. Bender and H.V. Klapdor, *Z. Phys.* A334 (1989) 177

- [38] J. Suhonen and O. Civitarese, *Phys. Lett.* B280 (1992) 191
- [39] F. Krmpotić, *Phys. Rev.* C48 (1993) 1452
- [40] K. Kume, H. Ejiri, K. Fushimi, R. Hazama, T. Kawasaki, V. Kunts, N. Kudomi, V. Malishko, K. Matsuoka, K. Nagata, H. Ohsumi, K. Okada, H. Sano, T. Shibata, T. Shima, J. Tanaka and Yu. Zdesenko, *Osaka University annual report (1992)* p. 20
- [41] S. Raman, T.A. Walkiewicz, S. Kahane, E.T. Journey, J. Sa, Z. Gácsi, J.L. Weil, K. Allaart, G. Bonsignori and J.F. Shriner Jr., *Phys. Rev.* C43 (1991) 521
- [42] M. Guttman, E.G. Funk and J.W. Mihelich, *Nucl. Phys.* 64 (1965) 401